

## Preparation of Chromatic Beautifying Coating for Asphalt Pavements Based on Response Surface Methodology

Hongjun Jing<sup>1,2</sup>, Yefan Lei<sup>1,2,\*</sup>, Changliang Zhao<sup>3</sup>, Chenggang Wang<sup>3</sup> and Xiao Mu<sup>4</sup>

<sup>1</sup>College of Architecture and Civil Engineering, Xi'an University of Science and Technology, Xi'an 710054, China

<sup>2</sup>Road Engineering Research Center of Xi'an University of Science and Technology, Xi'an 710054, China

<sup>3</sup>Maintenance Center of Yan'an Highway Bureau, Xi'an 716000, China

<sup>4</sup>Zhengzhou Business University, Zhengzhou 451200, China

Received 13 August 2024; Accepted 28 November 2024

### Abstract

A beautifying coating that can improve the color differences of pavements was prepared in this work to improve road aesthetics and the traveling safety of drivers and to solve color differences problems of asphalt pit roads after repair. First, E51 epoxy resin and BS-104-2 emulsion acrylic resin were used as the major film formation base material, to which three color fillings (e.g., titanium dioxide, matting powder, and wollastonite powder) and other accessory ingredients were added to form the base coating. The interactive influences of the three color fillings on the glossiness and covering power of the coating were investigated by response surface methodology, and the mixing ratio of the beautifying coating was optimized. Second, beautifying coatings with different color levels were prepared by controlling the contents of different color pastes. Finally, the basic properties of the optimized beautifying coatings were tested. According to test results, the optimal mixing ratio under the interactive effect of glossiness and covering power of the coating is as follows: film formation base material: titanium dioxide: matting powder: wollastonite powder = 112.3:73.7:21.2:39.9. The color paste contents for asphalt pavement with Red-Green-Blue (RGB) I, II, and III coatings are 0.07, 0.04, and 0.02 g, respectively. After exposure to strong light for 100 h, the RGB chromatic value of the coatings tended to be stable, indicating that coatings have color retention capacity and age resistance to some extent after the addition of pigments. After the coatings are applied to test roads, the coatings could decrease the color differences of the pavement effectively. The prepared chromatic beautifying coating for pavements has important significances to enhance traveling safety and the road aesthetics of asphalt pavement.

*Keywords:* Color differences of pavement, Glossiness, Covering power, Pigment, Beautifying coating

### 1. Introduction

Road construction faces greater challenges than it did before with the rapid development of the traffic industry. The frequent occurrence of various pavement diseases in recent years has seriously affected the normal service of roads. The traveling comfort and safety of drivers are both threatened to different extents. Protecting asphalt pavement against diseases has become the priority in the road engineering field to guarantee the sustainable development of road construction [1].

At present, pit disease accounts for a high proportion of issues in asphalt pavement maintenance, and different maintenance schemes have been developed accordingly [2]. Materials such as hot-mix asphalt mixture, cold-mix asphalt mixture [3], and polymer materials are being optimized and improved continuously. Meanwhile, technologies such as fog sealing layer, chip sealing layer, micro-surface, slurry sealing layer, thin-layer coating, and hot in-place recycling are becoming increasingly mature [4]. Nevertheless, relevant maintenance schemes mainly focus on emergency countermeasures due to limitations posed by practical construction conditions and different repair levels of pit pavement [5]. Moreover, asphalt pavement is exposed for a long time and will suffer different degrees of wear with the increase in service time. The surface color also changes from deep black to gray. The color of the newly repaired pit

pavement may also differ significantly from the original pavement. Such difference not only influences drivers' fast accurate judgment of pavement diseases but may also affect also their decision-making behaviors and vision [6]. Moreover, obvious color differences may influence the psychology of drivers [7], which easily causes them to decelerate or avoid vehicles, thus further increasing traffic risks. Additionally, the obvious color differences on pavement may decrease the overall coordination of roads, which disagrees with the original intention of beautiful design [8] and causes uncomfortable visual feelings.

Therefore, solving color differences between new and old pavements after the repair of asphalt pit pavements has become an urgent challenge. To decrease color differences produced by old asphalt pavement and improve driving safety and road aesthetics, this study proposed a beautifying coating with good comprehensive performances for old asphalt pavement with color differences and investigated its performance.

### 2. State of the Art

Most pavements are mainly black, white, and gray. The development of colorful pavement provides a new direction for the selection of pavement colors. Ning et al. [9] proposed a color asphalt pavement sprayed with anti-tire trace sealing resin emulsion on the road surface, which significantly

\*E-mail address: yefanley@163.com

ISSN: 1791-2377 © 2024 School of Science, DUTH. All rights reserved.

doi:10.25103/jestr.176.12

improved the durability of the road surface. Studies on pavement colors mainly focus on colorful asphalt pavement, and the chosen aggregates are mainly light colored or have different colors. Pigments are mainly prepared on the basis of three primary colors, which does not apply to the gray-black of old asphalt pavement. Nowadays, colorful asphalt pavement is mainly applied to landscape roads and pedestrians, but they do not apply to heavy-loaded roads.

Coating materials have been extensively applied to road engineering for their tremendous advantages. Scholars have studied the coating materials of asphalt pavement thoroughly and have successfully overcome many difficulties over the middle and long term of road construction [10,11]. To address the problem of urban heat island, scholars have prepared different kinds of heat-reflecting coatings by using different reflective pigments. Sha et al. [12] designed a special solar heat-reflective coating, which reduced the surface temperature of asphalt pavement by about 10 °C. Anak et al. [13] used waste tiles as coating materials to relieve urban heat island. This new coating can lower the pavement temperature by 4.4 °C and serve as a natural coolant to the pavement after rainfall. However, the high reflectance of the above coatings in the surrounding environment may make drivers dizzy and affect their visual comfort, which has potential safety risks.

To improve the anti-icing performance of pavement at low temperatures, scholars prepared different super-hydrophobic coatings [14,15] by using fluorinated polymer, silane materials, and nanomaterials to strengthen hydrophobicity and waterproofness of surfaces. Lu et al. [16] prepared hydrophobic modified TiO<sub>2</sub> by using the PTFE cladding method and prepared epoxy resin modified organic silicon resin by using the blending method, which supplied raw material supports to self-cleaning pavement paints. Although super-hydrophobic coatings have self-cleaning characteristics, the accumulated dirt and pollutants may still adhere to the coating surface in some cases, decreasing the beauty and functions of coatings.

On this basis, existing pavement materials were summarized in this study with references to experiences in asphalt pavement maintenance. With epoxy resin and acrylic resin as the main film-forming materials, the interactive effects of consumptions of titanium dioxide, matting powder, and wollastonite powder on the covering power and glossiness of the coating were explored by using response surface methodology (RSM). The mixing ratio of beautifying coating was optimized, and a beautifying coating that can decrease color differences of pavement after pit repair was developed. This work provides a new idea to realize consistent colors between repaired pit pavement and the original pavement.

The remainder of this study is organized as follows. Section 3 elaborates the composition of the coating, test method, and design of the mixing ratio for the colorful filler test. Section 4 analyzes the covering power and glossiness of colorful fillers after optimization by RSM, obtaining mixing ratios of pigments for pavement with different color levels. The aging resistance performances of the coating were analyzed, and the repair effect after application of the coating was evaluated. Section 5 summarizes relevant conclusions.

### 3. Methodology

#### 3.1 Raw materials

##### 3.1.1 Film formation base material

Film formation base material is the major chemical substance in the chromatic beautifying coating of pavement. It is the skeleton structure of the coating and is mainly subjected to pressure and friction force from the pavement loads. The film formation base material of pavement coating is composed of resins (e.g., epoxy resin and acrylic resin) and non-volatile reactive diluents. The E51-type epoxy resin and the modified BS-104-2 emulsion-type acrylic resin were used as the base solution of epoxy, to which constant volumes of diluent and resin base solution were added and stirred for 1 h. After cooling, flexibilizer, 593 curing agent, and DMP-30 accelerant were added successively. The mixture was then placed in a vacuum oven under 25 °C, thus obtaining the epoxy resin base (EPM).

On the basis of early studies of the research team [17], the mass ratio of EPM was gained after comprehensive analysis. The results are listed in Table 1.

**Table 1.** EPM ratio

Epoxy resin base fluid (%)	Flexibilizer (%)	Diluent (%)	Curing agent (%)	Accelerator (%)
100	15	30	60	6

##### 3.1.2 Colorful fillers

The covering power and glossiness of the coating were improved by using three kinds of colorful fillers: titanium dioxide, wollastonite powder, and matting powder. The relative density of titanium dioxide is 3.9–4.2 g/cm<sup>3</sup>, the refractive index is 2.76, the maximum particle size is 0.3nm, and the coloring strength is 1650–1900. The wollastonite powder was acquired using coal ash from a power plant through wet processing, with a refraction coefficient of 0.4, a density of 1.86 g/cm<sup>3</sup>, and a thermal expansion coefficient of 2. The SAK-2000 type matting powder was applied, with a shading coefficient of 1.47, an oil absorption range of 210–260, and a porosity of 1.8 ml/g.

##### 3.1.3 Other accessory ingredients

The KH-570 silane coupling agent and 3016-type defoamer were chosen. The density of KH-570 silane coupling agent was 1.04 g/ml, the shading rate was 1.429, and the purity was more than 99 %. The density of the 3016-type defoamer ranges from 0.87 g/ml to 0.93 g/ml, and silicon-containing sol was used to decrease bubbles during the operation of mechanical equipment and synthesis of coating materials.

##### 3.1.4 Color pastes

Cellulose Acetate Butyrate (CAB) high-temperature-resistant transparent nanocolor pastes of Sanyuan New Material Band were chosen, which had good universality. The technical indexes are listed in Table 2.

**Table 2.** Technical indexes of color paste

Appearance	Viscosity 25° C (mPa s)	PH value	Particle size (nm)
Black liquid	2000-3000	7-10	≤200

#### 3.2 Experimental method

##### 3.2.1 Beautifying coating preparation

After the EPM and pigments were stirred, the coating paints were obtained. The coating paints of different color grades were prepared by adjusting curing temperatures. With

reference to *Performance Test Method of Resin Casting Body*, paints were poured into a Teflon template to prepare dumbbell-shaped specimens. The specimens were placed in

a drying oven, cured for 8 h, and then tested. The specific preparation process and performance test of the beautifying coating paints are shown in Fig. 1.

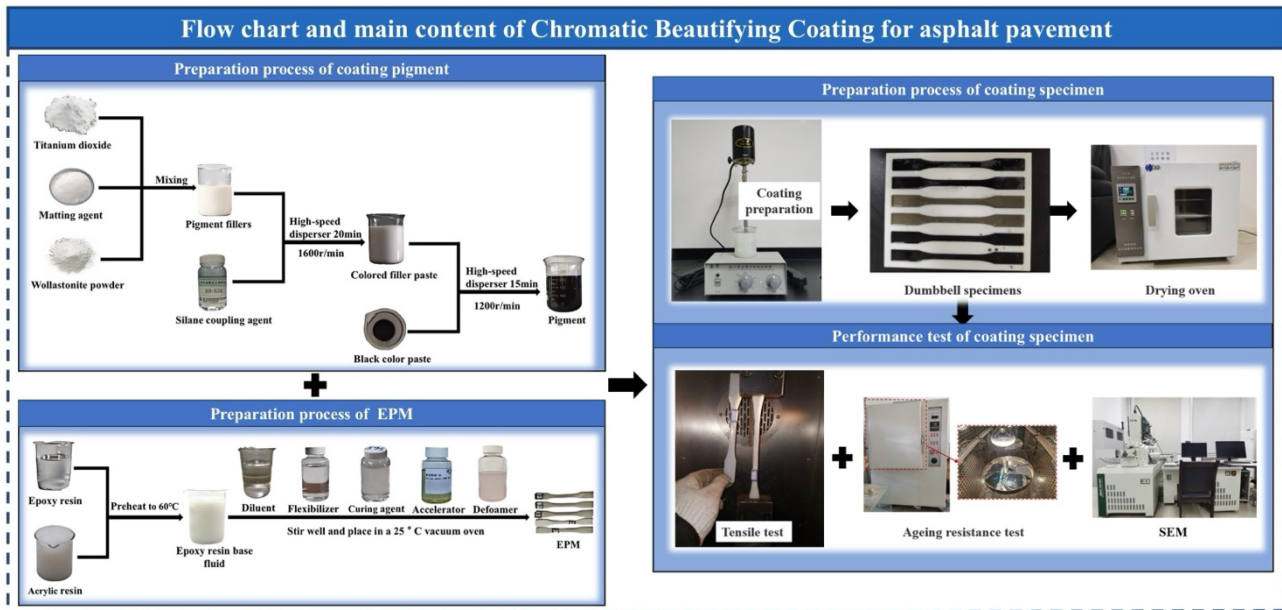


Fig. 1. Flow chart and main content of coating preparation

### 3.2.2 Aging resistance test

The color retention capacity of the coating was evaluated by analyzing color changes after the aging resistance test. The indoor ultraviolet aging of the coating was simulated by using the GT-7035-UB yellowing resistance test. The illumination intensity and exposure time of the instrument were  $10.76 \text{ W/m}^2/\text{nm}^{-1}$  and 100 h, respectively. The temperature in the test tank was maintained at  $40^\circ\text{C}$ , and the illumination distance was maintained at 40 cm for the artificial accelerated aging test.

### 3.2.3 Tensile test

The service performances of the coating after light aging were characterized through tensile strength test of the drawing test samples. The tensile test of the coating was carried out by using the universal tester. The test temperature was set at  $0^\circ\text{C}$ , and the samples were stretched out slowly at a uniform speed ( $10 \text{ m/min}$ ). The strength of the stretching test specimens was tested by reading the maximum tension and breaking length of the specimens.

### 3.2.4 Scanning electron microscope

Scanning electron microscope (SEM) test of the coating was carried out by using a JSM-7610F ultra-high resolution thermal field-emission scanning electron microscope. The surface morphology and breaking surface of the coating were observed, and the dispersion degree of pigments in the coating was analyzed.

## 3.3 Design of test mix proportion

### 3.3.1 Single-factor tests

A total of 200 g of film formation base material was chosen, to which different amounts of titanium dioxide, matting powder, and wollastonite powder were added to explore the

influences of different colorful fillers on the covering power and glossiness of the coating.

### 3.3.2 Multi-factor mix design

The optimal mixing ratio of pigments in the chromatic beautifying coating for old asphalt pavement was determined by adding matting powder, wollastonite powder, and titanium dioxide. In this study, the test was optimized by RSM [18]. On the basis of the BBD principle, the midpoint of each side of the encoding cube was chosen as the test point. Quadratic polynomial fitting was carried out on the test results of 17 test points.

The interactive influences of matting powder, wollastonite powder, and titanium dioxide on the covering power and glossiness of chromatic beautifying coating of asphalt pavement were analyzed quickly and accurately through the quadratic regression model. The relationships between evaluation indexes and different factors were established. The basic equation of RSM is shown as follows:

$$y = \beta_0 + \sum_{i=1}^k \beta_i x_i + \sum_{i=1}^k \sum_{j=1}^k \beta_{ij} x_i x_j + \sum_{i=1}^k \beta_{ii} x_i^2 + \varepsilon \quad (1)$$

Where  $y$  is the evaluation index estimates;  $\varepsilon$  is the experimental error;  $\beta$  is the coefficient estimates; and  $x$  is the factor.

## 4. Result Analysis and Discussion

### 4.1 Test results and discussion of covering power and glossiness of colorful fillers for coating

#### 4.1.1 Single-factor analysis results

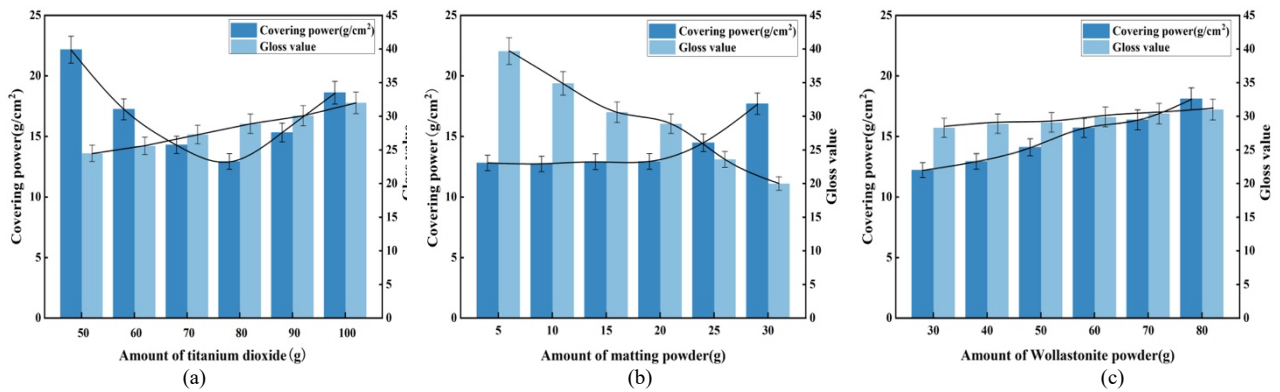


Fig. 2. Influence curve of different colorful filler amount on the covering power and glossiness (a) the amount of titanium dioxide (b) the amount of matting powder (c) the amount of wollastonite powder

According to the results in Fig. 2(a), With the increase in the content of titanium dioxide, the covering power of the coating decreases first and then increases. The covering power of the coating reaches the minimum when the content of titanium dioxide is 80 g. Under this circumstance, the coating shows the strongest covering ability. With the increase in the content of titanium dioxide, the glossiness value of the coating increases gradually, while the reflection of light decreases gradually [19].

Fig. 2(b) shows that matting powder has slight influences on covering power when its content is 0–20 g. After the content of matting powder exceeds 20 g, the covering power increases gradually, but the covering ability declines. Hence, the coating achieves the strongest covering ability when the content of matting powder is 20 g. With the increase in the content of matting powder, the glossiness value of the coating decreases gradually, and the reflection of light increases continuously.

Fig. 2(c) shows that with the increase in the content of wollastonite powder, the glossiness value of the coating increases slowly, and the reflection of light does not change obviously. Therefore, wollastonite powder basically has no influence on the glossiness of the coating. Within the consumption range of wollastonite powder, the glossiness of the coating is always kept lower than 30.

In sum, the content ranges of titanium dioxide, matting powder, and wollastonite powder were 70–90, 20–30, and 30–50 g, respectively.

#### 4.1.2 Optimization design of covering power and glossiness of colorful fillers for coating

##### 4.1.2.1 Establishment of response equation and significance analysis

Table 3. BBD independent parameter and its code

Parameter	Code	Code parameter level		
		-1	0	1
Titanium dioxide	x <sub>1</sub>	70	80	90
Matting powder	x <sub>2</sub>	20	25	30
Wollastonite powder	x <sub>3</sub>	30	40	50

Dimensionless linear encoding was carried out to test the parameters (Table 3). The multiple regression model equation for the response value and the independent variables was fitted by the least squares method. The optimal design scheme is shown in Table 4. The quadratic model with the maximum R<sup>2</sup> was chosen. The quadratic regression model is fitted as follows:

$$y_1 = 12.23 - 0.8937x_1 + 0.19x_2 + 0.7812x_3 - 0.075x_1x_2 - 1.4225x_1x_3 - 0.07x_2x_3 + 0.8532x_1^2 + 0.2707x_2^2 + 0.6223x_3^2 \quad (2)$$

$$y_2 = 23.58 + 1.29x_1 - 4.27x_2 + 0.3625x_3 - 0.425x_1x_2 + 0.15x_1x_3 + 0.025x_2x_3 - 0.015x_1^2 - 0.86x_2^2 - 0.165x_3^2 \quad (3)$$

Table 4. Optimal design scheme based on the RSM

Run	x <sub>1</sub>	x <sub>2</sub>	x <sub>3</sub>	Covering power	Glossiness
1	90	20	40	12.32	24.4
2	80	25	40	12.14	20.4
3	80	20	30	12.00	23.5
4	80	30	30	12.40	30.2
5	80	30	50	14.10	19.6
6	70	20	40	13.88	23.6
7	80	25	40	12.28	25.4
8	90	30	40	12.67	22.1
9	70	30	40	14.53	23.6
10	90	25	30	12.55	23.8
11	80	25	40	12.11	23.4
12	80	20	50	13.98	21.7
13	90	25	50	12.99	20.8
14	70	25	50	15.70	28.2
15	80	25	40	12.39	27.2
16	70	25	30	13.57	19.5
17	80	25	40	12.21	28.9

The variance analysis of regression models is shown in Table 5, where the F value is 56.32 and 284.02, while the P value is <0.0001, indicating that models 1 and 2 are both significant. The misfit degree (F value) is 5.10 and 5.49, while the P value is 0.0747 and 0.0667 (>0.05), indicating that models have insignificant misfit degrees. According to the regression analysis results, the model can analyze and predict the relationship between response value and factors well [20]. In Table 5, the primary term coefficients (x<sub>1</sub>, x<sub>2</sub>, and x<sub>3</sub>) of response models 1 and 2 are all lower than 0.05, indicating that titanium dioxide, matting powder, and wollastonite powder can all influence the covering power and glossiness significantly. According to the primary term coefficients in Eqs. (2) and (3), matting powder and wollastonite powder can promote covering power positively; titanium dioxide and wollastonite powder can promote glossiness positively; while matting powder decreases the glossiness.

The P value of the interaction terms (x<sub>1</sub>x<sub>2</sub> and x<sub>2</sub>x<sub>3</sub>) of the response model 1 is higher than 0.05, and the P value of x<sub>1</sub>x<sub>3</sub> is lower than 0.05. This finding reflects that no significant interaction occurs between titanium dioxide and matting powder as well as between matting powder and wollastonite powder in the test range. Titanium dioxide and wollastonite powder show a significantly collaborative effect

on weakening the increase in covering power. In the response model 2, the P values of  $x_1x_2$  and  $x_2x_3$  are less than 0.05, and the P value of  $x_1x_3$  is higher than 0.05, indicating a significant interaction between titanium dioxide and matting

powder as well as between matting powder and wollastonite powder. Titanium dioxide and wollastonite powder show a significantly collaborative effect in the weakening reduction of glossiness.

Table 5. ANOVA of the regression model

Response		SS	DF	MS	F-value	P-value	significance
Response 1: Covering power	Model	17.80	9	1.98	56.32	< 0.0001	significant
	X <sub>1</sub>	6.39	1	6.39	182.03	< 0.0001	
	X <sub>2</sub>	0.2888	1	0.2888	8.23	0.0241	
	X <sub>3</sub>	4.88	1	4.88	139.09	< 0.0001	
	X <sub>1</sub> X <sub>2</sub>	0.0225	1	0.0225	0.6409	0.4497	
	X <sub>1</sub> X <sub>3</sub>	0.7140	1	0.7140	20.34	0.0028	
	X <sub>2</sub> X <sub>3</sub>	0.0196	1	0.0196	0.5583	0.4793	
	Residual	0.2457	7	0.0351	-	-	
	Lack of Fit	0.1948	3	0.0649	5.10	0.0747	not significant
	Pure Error	0.0509	4	0.0127	-	-	
Cor Total	18.04	16	-	-	-		
Response 2: Glossiness	Model	164.51	9	18.28	284.02	< 0.0001	significant
	X <sub>1</sub>	13.26	1	13.26	206.06	< 0.0001	
	X <sub>2</sub>	146.20	1	146.20	2271.78	< 0.0001	
	X <sub>3</sub>	1.05	1	1.05	16.33	0.0049	
	X <sub>1</sub> X <sub>2</sub>	0.7225	1	0.7225	11.23	0.0122	
	X <sub>1</sub> X <sub>3</sub>	0.0900	1	0.0900	1.40	0.2756	
	X <sub>2</sub> X <sub>3</sub>	0.0025	1	0.0025	0.0388	0.8494	
	Residual	0.4505	7	0.0644	-	-	
	Lack of Fit	0.3625	3	0.1208	5.49	0.0667	not significant
	Pure Error	0.0880	4	0.0220	-	-	
Cor Total	164.96	16	-	-	-		

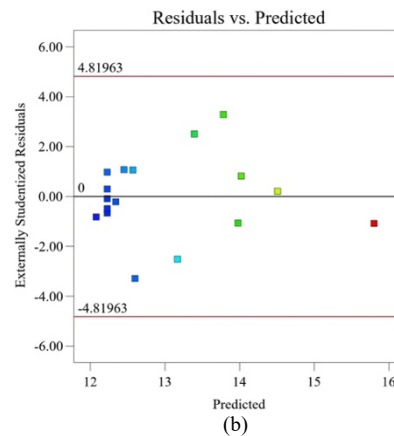
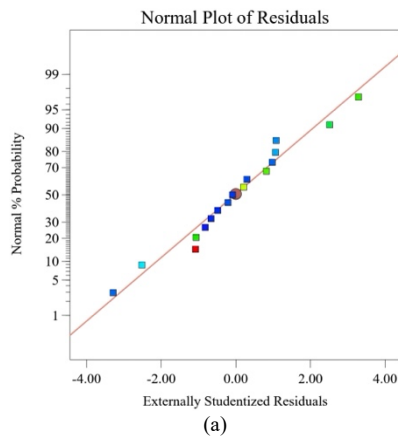
In Table 6, R<sup>2</sup> of the response model 1 is 0.9864. Hence, less than 2% of total variance cannot be interpreted by the response model 1. On the basis of the above parameter analysis results, the factors in the response process can be characterized by this response model. R<sup>2</sup> of the response model 2 is 0.9973, and the model is extremely significant on the 99% confidence level. On the basis of the above parameter analysis results, the response model 2 can be used to characterize factors in the response process. Meanwhile, the test results are analyzed and predicted.

4.1.2.2 Model suitability test

The residual normal probability diagram is shown in Figs. 3(a) and (b). The distribution of data points is approximately a straight line, indicating that the residual errors have a normal distribution and conform to requirements. The standardized residual error and fitting value are shown in Figs. 3(c) and (d). All test points are in the control line, without obvious anomalies. The following diagram shows that residual errors have a random distribution and the residual errors are unrelated to the fitting value. Hence, this model chooses factors reasonably, guaranteeing that the simulated covering power and glossiness of the colorful fillers of the coating are close to real test results [21].

Table 6. Fit statistics of response model

Response	Y <sub>1</sub>	Y <sub>2</sub>
R <sup>2</sup>	0.9864	0.9973
Adjusted R <sup>2</sup>	0.9689	0.9938
Predicted R <sup>2</sup>	0.8228	0.9640



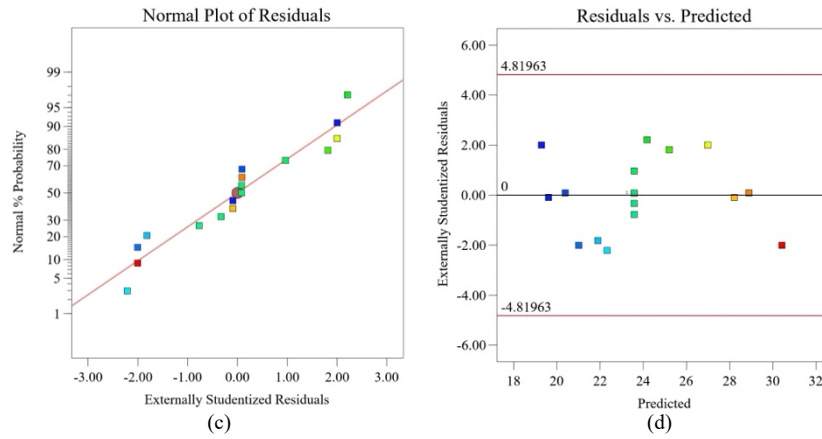


Fig. 3. Residual plot of quadratic regression model

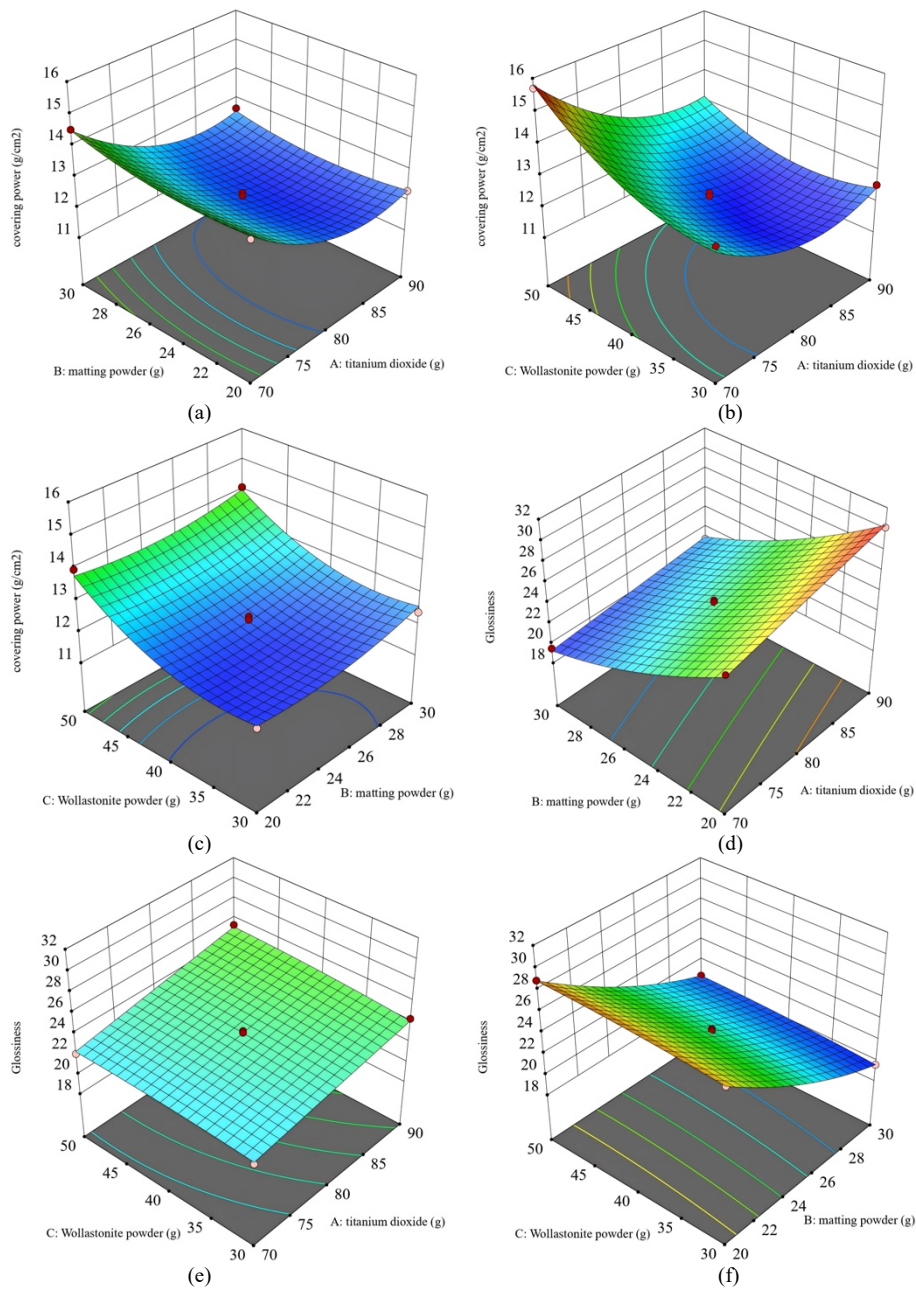


Fig. 4. Effects of titanium dioxide, matting powder, and wollastonite powder on covering power and glossiness

#### 4.1.2.3 Application of response surface

The interactive effects of titanium dioxide and matting powder, titanium dioxide and wollastonite powder, and matting powder and wollastonite powder on covering power

are shown in Figs. 4(a)–(c). All response surfaces are curved surfaces [22]. The interactive effect of titanium dioxide and wollastonite powder on the covering power is the most obvious. With the decrease in the titanium dioxide content

and the increase in the wollastonite powder content, the covering power increases continuously. Moreover, the wollastonite powder content influences covering power more. The covering power is positively related to the titanium dioxide content. When the titanium dioxide content is fixed, the covering power does not change obviously with the changes in matting powder content. Therefore, the titanium dioxide content influences the covering power more than wollastonite powder does. With the increase in the contents of matting powder and wollastonite powder, the covering power increases continuously. When the wollastonite powder content is fixed, the covering power does not change obviously with the change of matting powder content. Therefore, wollastonite powder content influences covering power more than matting powder does. To sum up, the interactive effects of titanium dioxide, wollastonite powder, and matting powder can influence the covering power of colorful fillers of the coating to some extent, with titanium dioxide having the greatest influence, followed by wollastonite powder and matting powder.

The interactive effects of titanium dioxide and wollastonite powder, titanium dioxide and matting powder, and matting powder and wollastonite powder on glossiness are shown in Figs. 4(d)–(f), where the graph response surface has a curved surface shape. In Fig. 4(e), the response surface is close to a plane. In Fig. 4(d), the interactive effect of titanium dioxide and wollastonite powder on covering power is relatively obvious. With the decrease in the titanium dioxide content and the increase in the wollastonite powder content, glossiness declines continuously and matting powder content influences the glossiness more. The response surfaces in Fig. 4(e) are approximately planar, which is why the influences of titanium dioxide and wollastonite powder on glossiness are basically consistent. With the increase in the matting powder content and the decrease in the wollastonite powder content, the glossiness decreases gradually. Hence, the matting powder content influences glossiness more. On the basis of the above analysis, the interactive effect of titanium powder, matting powder, and wollastonite powder can affect covering power and glossiness to some extent. Specifically, matting powder influences covering power and glossiness the most, followed by titanium dioxide and wollastonite powder. The optimal conditions for glossiness are 79.8 g of titanium dioxide, 29.3 g of matting powder, and 47.5 g of wollastonite powder. Under the optimal conditions, the glossiness reaches 20.716.

#### 4.1.3 Parameter optimization of the ratio of colorful fillers for coating

When the coating is applied to pavement, the solar rays reflected in the coating will be transmitted to the eyes of drivers, resulting in glare and visual fatigue, thus further causing safety problems. Therefore, the glossiness of the coating should be lower than  $30^\circ$  and  $y_2 \leq 30$  according to standards (GB/T9754-2007).

$y_1 = f_i(x_1, x_2, x_3)$  is the ideal point of the model, and  $Z_i$  is introduced as any point on the curved surface. The optimal model is built as follows:

$$\min \varphi(z) = Z_i - f_i \quad (4)$$

$$s.t. \begin{cases} y_2 \leq 30 \\ 70 \leq x_1 \leq 90, 20 \leq x_2 \leq 30, 30 \leq x_3 \leq 50 \end{cases} \quad (5)$$

It is solved by combining Eqs. (4) and (5), deriving the optimal mixing ratio of colorful fillers: 73.7 g of titanium dioxide, 21.2 g of matting powder, and 39.9 g of wollastonite powder.

#### 4.2 Pigment ratio results of asphalt pavement with different color levels

White powder slurry of colorful fillers was acquired through the optimal mixing ratio of components in the colorful fillers for coating. According to asphalt pavement of different color levels, different proportions of black paste were added to the white powder slurry of colorful fillers to form the final pigments. The final pigments were stirred with EPM to prepare beautifying coatings for asphalt pavements with different color levels.

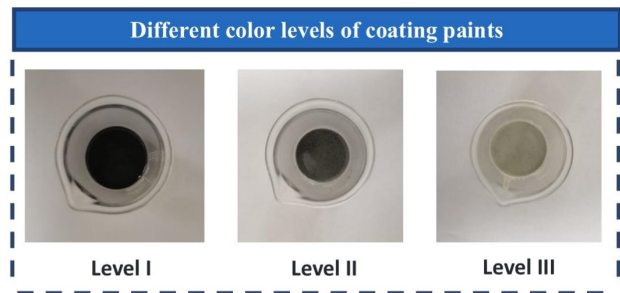


Fig. 5. Coatings with different color levels

The colors of old asphalt pavements are divided into three levels according to RGB values. Different amounts of color pastes were added to prepare beautifying coatings with three color levels (Fig. 5). The RGB values of coatings with three color levels were tested by using a CS-410 spectrophotometer; the measured RGB values are in the range of different color levels. The mixing ratios of coating colors are shown in Table 7.

Table 7. Amount ratio of different color level coatings

Level	RGB	Coating:black color paste	RGB measurements
Level I	70-89	100g: 0.07g	77,76,77
Level II	89-105	100g: 0.04g	96,97,95
Level III	105-123	100g: 0.02g	119,121,122

#### 4.3 Coating aging resistance test results and discussion

##### 4.3.1 Analysis of color change of coating before and after adding pigment

Coatings for asphalt pavements at RGB I, II, and III levels were prepared. The prepared paints were coated onto 10 cm × 10 cm stainless steel plates, respectively. After curing at room temperature, the indoor simulated aging test was carried out to observe the color change and apparent morphology after aging for 12 and 100 h.

The aging resistance test results after paints of different color levels were coated onto stainless steel plates are shown in Fig. 6. Clearly, the apparent colors of the coatings at different color levels change slightly after aging for 12 h. Colors of coatings at different color levels faded after aging for 100 h. With the increase in the aging time, the glossiness of coating surfaces decreased, accompanied with the occurrence of white powder film. However, no pulverization was observed on the coating surface. After 100 h of the indoor aging test, the coatings of different color grades did not crack and peel off, which showed that the coating had good aging resistance.

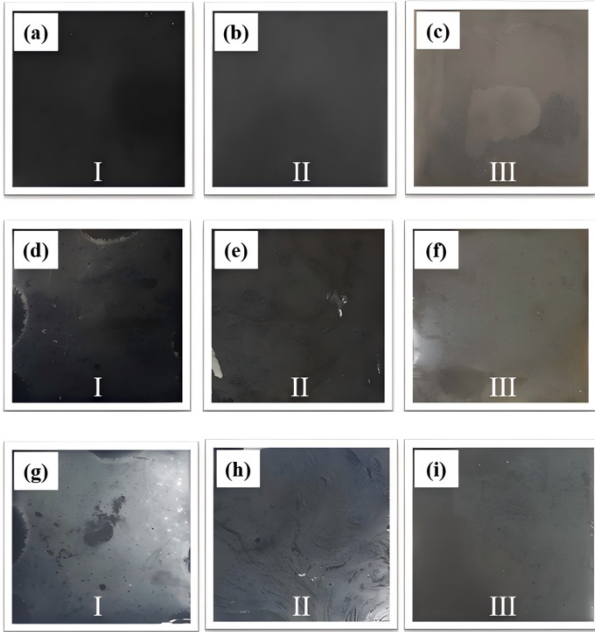


Fig. 6. Effect of different color coatings on steel plates and its result analysis (a) Level I coating effect, (b) Level II coating effect, (c) Level III coating effect, (d) Level I 12 h after aging, (e) Level II 12 h after aging, (f) Level III 12 h after aging, (g) Level I 100 h after aging, (h) Level II 100 h after aging, (i) Level III 100 h after aging.

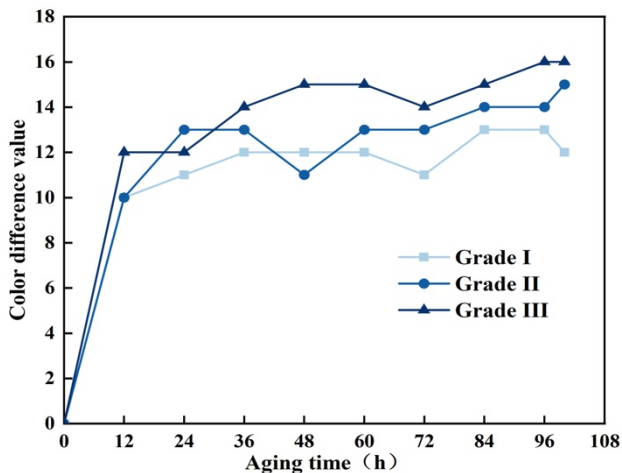


Fig. 7. Color difference changes of different aging specimens

The RGB values of coatings under different aging times were measured by using the CS-410 spectrophotometer. RGB differences between specimen surface colors and the original colors were recorded. The measurement results are shown in Fig. 7. Clearly, the RGB values of coatings at different color levels presented linear relations over 12 h of the library aging simulation test, and the RGB differences increased at a uniform speed. At 12 h of aging, the growth rate of RGB differences of coatings at different color levels began to change. After 12 h of aging, the growth rate of RGB differences began to decrease. With the increase in the aging time, the RGB values of coatings at different color levels tended to be stable gradually. The measurement results show that coatings at different color levels can maintain colors to some extent.

The color changes of the coating specimens without colorful fillers before the color paste was added are compared and analyzed in Figs. 8(a) and 8(b). This condition reflects that the coatings have good stability after adding colorful fillers, which can decrease the yellowing

phenomenon. Moreover, coatings can resist ultraviolet rays, and the weather resistance of coatings is improved [23]. After color paste was added, a comparative analysis on colors of coating specimens without colorful fillers (Fig. 8[c]) and coating specimens with colorful fillers (Fig. 8[d]) was carried out. Clearly, the colors of the coating specimens with colorful fillers changed slightly. According to the test results, adding colorful fillers can cover coating surfaces to some extent and narrow the region that is directly exposed to lights and environmental factors, thus decreasing the possibility of color changes caused by external factors.

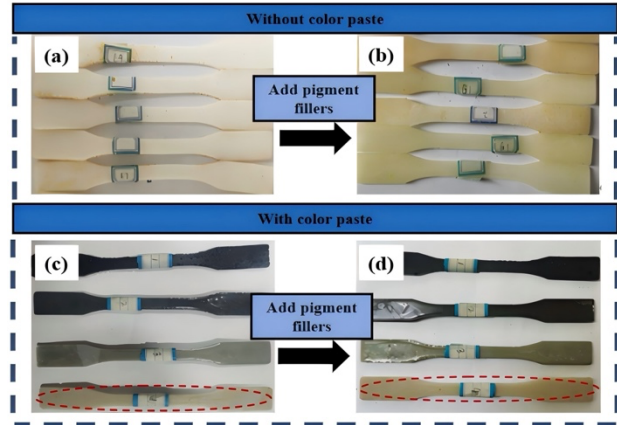


Fig. 8. Color changes of drawing specimens

#### 4.3.2 Analysis of coating tensile strength results

The tensile strengths of dumbbell-shaped specimens with and without pigments (Y-1 and N-1) before and after aging are tested, and the service performances of coatings after aging are analyzed. The test results are shown in Fig. 9.

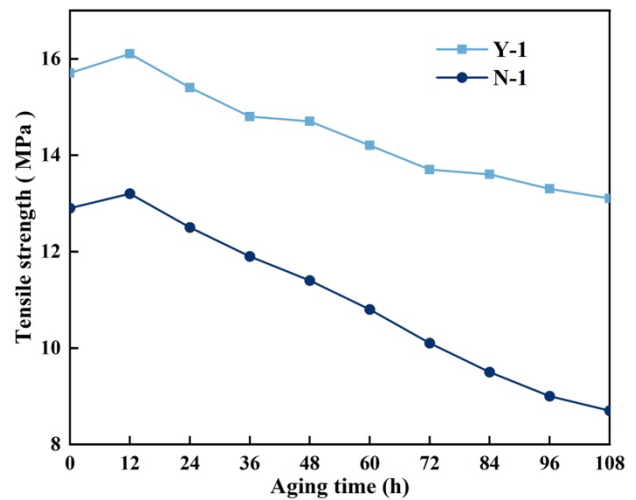


Fig. 9. Effect of light aging test on the tensile strength of coating material

Before 12 h of aging, tensile strength values of specimens N-1 and Y-1 both presented a rising trend. After 12 h of aging, their tensile strength values showed a trend of slowly decreasing with the increase in the aging time. This condition occurred because coatings experience oxidative degradation under long-term light aging and the chemical bonds in coating resins break, thus decreasing the performances of coatings. The tensile strength of specimens after aging of coating with pigments decreases to a small extent. This result occurs because titanium dioxide is the major component of titanium white powder in pigments. The excellent dispersion and covering of titanium dioxide can



reflect harmful light waves and absorb optical energy [24]. Coating energy is emitted as thermal energy, which improves the aging resistance of coatings. The test results show that the addition of pigments can improve the tensile strength of the coating material and also improve the durability and anti-aging ability of the coating.

#### 4.4 SEM test results and discussion

The microstructure of coating surfaces is shown in Figs. 10(a) and (b). When the amplification factor is 1000, several spiral chain-like connectors are formed on the coating surface, which can strengthen the coatings. Adding a silane coupling agent can disperse rough molecules on the paint surface uniformly and lower surface energy in the organic matrix, thus bringing good compatibility between pigments and film formation base material. As a result, the interaction of the phase interface is strengthened. When the amplification factor is 5000, no large bulking or bonding substances can be seen, indicating that fillers disperse in paints well. Figs. 10(c) and (d) show that the fracture surfaces of coatings are rough, showing abundant sawtooth structures and irregular fracture surfaces. Some pigment particles are highlighted on fracture surfaces. The particle distribution indicates that pigments disperse uniformly in the film formation base material.

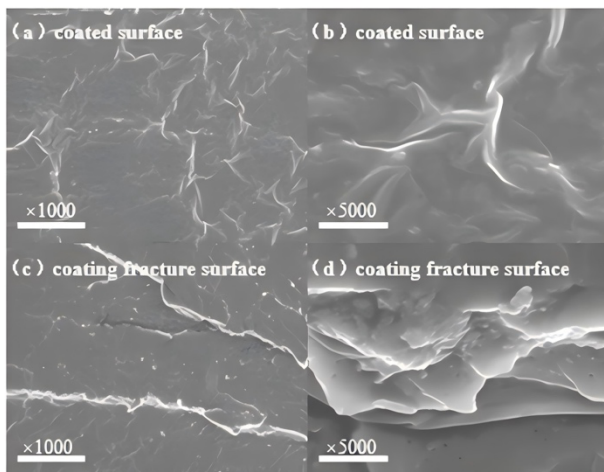


Fig. 10. SEM scanning diagram

#### 4.5 Remediation effect evaluation

The study area is located in Xi'an City, Shaanxi Province, which experiences heavy traffic loads and has many heavy-duty automobiles that operate at high speeds. The area of the chosen pit pavement for coating has a size of 3 m × 3 m. For a more intuitive comparison of the beautifying effect of coatings, the chosen pit pavement was divided into two parts: one is coated with coating, while the other is used as the control group.

Fig. 11 shows that from the perspective of human vision, the colors of the prepared coatings can mix with the original asphalt pavement colors well, without obvious color differences. This finding further verifies the repair effect of the beautifying coating. The coating colors were measured by a CS-410 spectrophotometer. Results show that the RGB difference ( $\Delta$ RGB) between the original pavement and the repaired pavement is lower than 10, thus reflecting the good effect of the beautifying coatings and their ability to decrease color differences in pavement.



Fig. 11. Comparison before and after repair

#### 5. Conclusions

Epoxy resin and acrylic acid are chosen as film formation base materials in this study to decrease the color differences of pavements after pit repair and improve driving safety and the beauty of pavements. Beautifying coatings that can decrease the color differences of pavement are prepared by adding different amounts of color paste. Three colorful fillers—titanium dioxide, matting powder, and wollastonite powder—are chosen according to the covering power and glossiness of coatings. The optimal mixing ratio of colorful fillers for coating is designed through RSM. The color changes and tensile performances after the aging resistance test of coatings are investigated, and the repair effect of the coatings is evaluated. The following major conclusions could be drawn:

(1) Single-factor tests are conducted to study the covering power and glossiness of coatings. The optimal ranges of titanium dioxide, matting powder, and wollastonite powder are 70–90, 20–30, and 30–50 g, respectively. According to RSM, the optimal mixing ratio of coatings is as follows: film formation base material: titanium dioxide: matting powder: wollastonite powder = 112.3: 73.7: 21.2: 39.9.

(2) The pavements are divided into three RGB levels (I: 70–89; II: 89–105; III: 105–123) according to the CS-410 spectrophotometer. Three kinds of beautifying coatings are prepared by adding 0.07, 0.04, and 0.02 g color paste, which are applied to asphalt pavements at different color levels.

(3) Adding colorful fillers can decrease the yellowing phenomenon of coatings effectively. No pulverization, cracking, and peeling are observed on the coatings after 100 h of aging. The color differences tend to be stable after 100 h of aging, thus reflecting that the coatings with pigments can retain colors and resist aging to some extent.

(4) The beautifying coatings are applied to test roads, showing a good coating effect. They not only decrease the color differences of pavement effectively but also improve driving safety and the beauty of pavements.

For pavements that have different color levels after repair, beautifying coatings under different mixing ratios of pigments and color paste are prepared. These coatings have good aging resistance and strong color maintenance. They solve the color differences of the pavement after maintenance and repair effectively. Nevertheless, follow-up monitoring over practical coating sites has not been carried out yet. Color changes after coating need to be tracked and recorded further in the future.

This is an Open Access article distributed under the terms of the Creative Commons Attribution License.



## References

- [1] M. Guo, R. Zhang, X. Du, and P. Liu, "A state-of-the-art review on the functionality of ultra-thin overlays towards a future low carbon road maintenance," *Engineering*, vol. 32, pp. 82-98, Jan. 2024, doi:10.1016/j.eng.2023.03.020.
- [2] R. Hafezzadeh, F. Autelitano, and F. Giuliani, "Asphalt-based cold patches for repairing road potholes - An overview," *Constr. Build. Mater.*, vol. 306, Nov. 2021, Art.no.124870, doi:10.1016/j.conbuildmat.2021.124870.
- [3] T. Wang *et al.*, "Advanced cold patching materials (CPMs) for asphalt pavement pothole rehabilitation: State of the art," *J. Clean. Prod.*, vol. 366, Sep. 2022, Art.no.133001, doi:10.1016/j.jclepro.2022.133001.
- [4] Y. Zhan *et al.*, "Pavement preventive maintenance decision-making for high antiwear and optimized skid resistance performance," *Constr. Build. Mater.*, vol. 400, Oct. 2023, Art.no.132757, doi:10.1016/j.conbuildmat.2023.132757.
- [5] Y. Xue *et al.*, "Road performance and mechanism of Hot in-place recycling asphalt mixture modified by direct-to-plant SBS," *Constr. Build. Mater.*, vol. 416, Feb. 2024, Art.no. 135122, doi:10.1016/j.conbuildmat.2024.135122.
- [6] M. Z. Hasan *et al.*, "Vision-language models can identify distracted driver behavior from naturalistic videos," *IEEE T. Intell. Transp.*, vol. 25, pp. 11602-11616, Oct. 2024, doi:10.1109/TBME.2011.2158315.
- [7] J. Niu, B. Liang, Y. D. Wong, S. He, and S. Wen, "Dynamic traffic safety risk assessment in road tunnel entrance zone based on drivers' psychophysiological perception states: Methodology and case-study insights," *Tunn. Under. Sp. Tech.*, vol. 147, May. 2024, Art.no.105677, doi:10.1016/j.tust.2024.105677.
- [8] M. Fathi and M. R. Masnavi, "Assessing environmental aesthetics of roadside vegetation and scenic beauty of highway landscape: preferences and perception of motorists," *Int. J. Environ. Res.*, vol. 8, pp. 941-952, Jul. 2014.
- [9] S Ning and S Huan, "Experimental study on color durability of color asphalt pavement," in *IOP Conf. Ser.: Mater. Sci. Eng.*, 2017, vol. 207, doi: 10.1088/1757-899X/207/1/012104.
- [10] G. Badin, N. Ahmad, and H. M. Ali, "Experimental investigation into the thermal augmentation of pigmented asphalt," *Physica A.*, vol. 551, Aug. 2020, Art.no.123974, doi:10.1016/j.physa.2019.123974.
- [11] H. Yu *et al.*, "The NOx Degradation Performance of Nano-TiO<sub>2</sub> Coating for Asphalt Pavement," *Nanomaterials*, vol. 10, May. 2020, Art.no.10050897, doi:10.3390/nano10050897.
- [12] A. Sha, Z. Liu, K. Tang, and P. Li, "Solar heating reflective coating layer (SHRCL) to cool the asphalt pavement surface," *Constr. Build. Mater.*, vol. 139, pp. 355-364, May. 2017, doi:10.1016/j.conbuildmat.2017.02.087.
- [13] N. A. Anak Guntor, F. M. Md Din, M. Ponraj, and K. Iwao, "Thermal performance of developed coating material as cool pavement material for tropical regions," *J. Mater. Civil Eng.*, vol. 26, pp. 755-760, May. 2014, doi:10.1061/(ASCE)MT.1943-5533.0000859.
- [14] Y. Li, A. Sha, Z. Tian, Y. Cao, X Li, and Z. Liu, "Review on superhydrophobic anti-icing coating for pavement," *J. Mater. Sci.*, vol. 58, Feb. 2023, doi:10.1007/s10853-023-08212-0.
- [15] Y. Cui, L. Zhang, C. Xing, and Y. Tan, "Anti-icing properties and application of superhydrophobic coatings on asphalt pavement," *Constr. Build. Mater.*, vol. 419, Mar. 2024, Art.no.135452, doi:10.1016/j.conbuildmat.2024.135452.
- [16] C. Lu, M. Zheng, J. Liu, R. Zhu, and Y. Su, "Characterization of self-cleaning pavement coatings with catalytic-hydrophobic synergistic effects," *Constr. Build. Mater.*, vol. 397, Sep. 2023, Art.no.132246, doi:10.1016/j.conbuildmat.2023.132246.
- [17] Q. Liu, M. Yang, H. Jing, Y. Jiang, and Y. Hu, "Preparation and performance of cementing materials for rapid maintenance of pavement potholes," *DYNA.*, vol.98, Jul. 2023, Art.no.259662063, doi:10.6036/10914.
- [18] M. A. Bezerra, R. E. Santelli, E. P. Oliveira, L. S. Villar, and L. A. Escalera, "Response surface methodology (RSM) as a tool for optimization in analytical chemistry," *Talanta*, vol. 76, pp. 965-977, Sep. 2008, doi:10.1016/j.talanta.2008.05.019.
- [19] J. Song *et al.*, "The effects of particle size distribution on the optical properties of titanium dioxide rutile pigments and their applications in cool non-white coatings," *Sol. Energy. Mat. Sol. C.*, vol. 130, pp. 42-50, Nov. 2014, doi:10.1016/j.solmat.2014.06.035.
- [20] L. Zhu, Z. Jin, Y. Zhao, and Y. Duan, "Rheological properties of cemented coal gangue backfill based on response surface methodology," *Constr. Build. Mater.*, vol. 306, Nov. 2021, Art.no.124836, doi:10.1016/j.conbuildmat.2021.124836.
- [21] K. Siamardi, "Optimization of fresh and hardened properties of structural light weight self-compacting concrete mix design using response surface methodology," *Constr. Build. Mater.*, vol. 317, Jan. 2022, Art.no.125928, doi:10.1016/j.conbuildmat.2021.125928.
- [22] G. E. P. Box and J. S. Hunter, "Multi-factor experimental designs for exploring response surfaces," *Ann. Math. Statist.*, vol. 28, pp. 195-241, Mar. 1957.
- [23] Y. Chen, R. Liu, and J. Luo, "Improvement of anti-aging property of UV-curable coatings with silica-coated TiO<sub>2</sub>," *Prog. Org. Coat.*, vol. 179, Jun. 2023, Art.no.107479, doi:10.1016/j.porgcoat.2023.107479.
- [24] J. H. Braun, A. Baidins, and R. E. Marganski, "TiO<sub>2</sub> pigment technology: a review," *Prog. Org. Coat.*, vol. 20, pp. 105-138, May. 1992, doi:10.1016/0033-0655(92)80001-D.